

AWOL: Analysis WithOut synthesis using Language

Silvia Zuffi¹ and Michael J. Black²

¹ IMATI-CNR, Milan, Italy
silvia@mi.imati.cnr.it

² Max Planck Institute for Intelligent Systems, Tübingen, Germany
black@tue.mpg.de

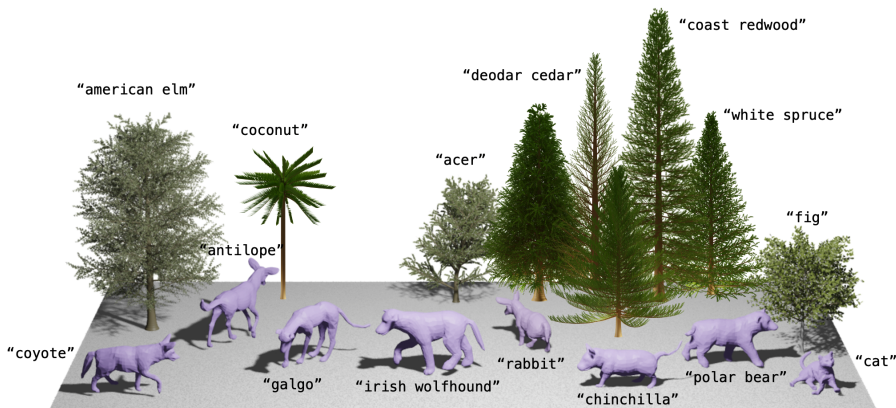


Fig. 1: Generated trees and animals. AWOL learns to generate animals and trees from text and images. We show examples for text-generated tree and animal species not seen during training (except for the cat).

Abstract. Many classical parametric 3D shape models exist, but creating novel shapes with such models requires expert knowledge of their parameters. For example, imagine creating a specific type of tree using procedural graphics or a new kind of animal from a statistical shape model. Our key idea is to leverage language to control such existing models to produce novel shapes. This involves learning a mapping between the latent space of a vision-language model and the parameter space of the 3D model, which we do using a small set of shape and text pairs. Our hypothesis is that mapping from language to parameters allows us to generate parameters for objects that were never seen during training. If the mapping between language and parameters is sufficiently smooth, then interpolation or generalization in language should translate appropriately into novel 3D shapes. We test our approach with two very different types of parametric shape models (quadrupeds and arboreal trees). We use a learned statistical shape model of quadrupeds and show that we can use text to generate new animals not present during training. In particular, we demonstrate state-of-the-art shape estimation of 3D dogs. This work also constitutes the first language-driven method for generating 3D trees. Finally, embedding images in the CLIP latent space enables us to generate animals and trees directly from images.

1 Introduction

We address the problem of generating new, realistic samples from various 3D shape models using language. The key idea is to relate language (e.g. names of dog breeds or types of trees) to the model’s parameters and then leverage language to generate shapes that were never seen during training. To make this possible, we leverage the shared latent space of large vision-language foundation models (VLM), like CLIP (Contrastive Language-Image Pretraining) [37]. Such models relate how objects appear in images to how we describe them with language. Since how objects appear is related to their 3D shape, we can assume that CLIP implicitly also relates object shape with language. Since models like CLIP are learned from large data corpora, VLM latent spaces are rich and dense; in other words, they know a lot about objects and their shape, but not explicitly. Given a small training set, we learn a mapping between the CLIP space and the shape parameters of various models. Finally, our central hypothesis is that the CLIP space is well-behaved such that interpolation or extrapolation in this space produce appropriate interpolation or extrapolation of the associated shape parameters. This allows us to exploit the general knowledge of a VLM to control the parameters of the shape model to produce novel shapes outside its training set. We test our hypothesis using two very diverse object classes, animals and trees, that use two very different generation processes. For animals, we use an analytic, statistical, parametric shape model, named SMAL⁺, that we introduce here as a new, extended version of previous models [23,41,64]. For trees, we use a procedural, non-differentiable, tree generator implemented as a Blender add-on [13]; this is very different from SMAL⁺. Trees are an interesting case because they are composed by thin structures (branches) and thin surfaces (leaves) that cannot easily be fit with the 3D implicit representations used in many current text-to-3D solutions. With our method, named AWOL, we generate trees and animals that are unseen during training and that are expressed as triangular meshes, thus supporting easy rendering and animation in graphics engines; see Fig. 1.

There is growing interest in generating 3D content with easy-to-use tools. An abundance of methods have been proposed to create 3D assets from simple text prompts, or single images [4,16,35,56]. Such methods are able to generate compelling rigid objects, with realistic appearance. Such models do not, however, produce articulated objects that are rigged for animation. With AWOL, we obtain animal models that share the same skeleton and mesh topology. This is important: a standardized 3D generation would allow easy motion transfer and facilitate analysis, promoting the application of 3D computer vision methods (i.e. 3D model-based articulated motion estimation) to the animal research and conservation fields.

Existing 3D parametric shape models for articulated subjects, like SMPL [28], for humans, or SMAL [62], for animals, are generative models for body shape, and consequently they are widely used to create 3D avatars, either by sampling the generative model, or by aligning the model to data [3,5,7,8,11,18,19,31,33,34,46,47,49,62,63]. Alignment is made possible by the differentiable nature of the mod-

els, which support reconstruction through the analysis-by-synthesis paradigm. While the SMPL model can arguably represent a large portion of the world population, given its large training set and uniqueness of the human species, the SMAL model has been trained on a small set of quadrupeds to represent animals from 5 different families (canine, equine, bovine, hippopotamids, and feline). As such, naively sampling the model shape space can produce non-existing animals that are often a mixture of more species. Sampling with family-specific shape priors (i.e. Gaussian distributions centered at the family mean shape variables) allows generating instances with realistic shape. However, as also illustrated in the paper [64], when aligned to data, the SMAL model can broadly represent species that are not present in its training set, for example representing a boar with a mane borrowed by lions, a long mouth from hippos, and bulky body from cows. The question then is: how can we generate animal species that are not in one of the five SMAL families without analysis-by-synthesis? The question is of broader application, as it regards the possibility of generalizing the generation of 3D assets given parametric models defined on a small set of samples. Identifying the manifold of realistic samples can be difficult: some regions of the space can correspond to shapes not seen during training, but realistic, while other regions can correspond to non-existing class instances. There is therefore a problem of realistic interpolation for data generation. In addition, shape models based on continuous latent spaces do not offer extrapolation capabilities, as in general their dimensions do not correspond to semantic deformations. While space transformations can be applied to identify axes with semantic meaning, this does not address the generalization principle, as how to move along these axes to generate new, realistic samples would still be not defined. In both the animals and trees models, the set of training samples is scarce. This limits the application of highly flexible generative models that are popular today, i.e. diffusion models. We employ Real-NVP [6], a generative model for highly structured data, characterized by a set of explicit transformations defined through a cascade of layers that selectively couple the different dimensions of the input data by means of binary masks. While the model has been used for text-to-3D generation before [44], using fixed masks, here we show that learning the binary masks improves performance, and, in particular for the animals model, add realistic relative scaling to the predicted shapes.

In summary, our contributions are: a new 3D parametric shape model for animals, which includes more species than previous models; a method to generate 3D rigged animals from text or images; a method to generate 3D trees from text or images, which can output a triangular mesh with fine branches and leaves details.

2 Related Work

Text-to-3D Our work is related to text-driven model-based 3D content creation systems. An early example is BodyTalk [45], which correlates textual shape attributes with transformed dimensions of the SMPL shape space. Semantify [12]

also addresses the problem of controlling the SMPL body model with shape attributes, but exploiting CLIP [37]. Recent work uses text to control 3D face generation [54]. In the past few years, an abundance of methods has addressed the text-driven generation of images [10, 38–40, 42, 43], and more recently 3D objects [4, 14, 16, 29, 51, 56]. Training is often based on the similarity between textual queries and rendered 3D shapes when encoded in a joint latent space (i.e. CLIP), with the gradient back propagated through a differentiable renderer. Many methods are thus based on differentiable 3D neural representations, often Neural Radiance Field (NeRF) [30], with a few mesh-based exceptions [26, 50]. Directly regressing a 3D triplane representation speeds up the text-to-3D generation [24]. Recent methods overcome the scarcity of 3D data by exploiting 2D losses. DreamFields generates open-set 3D objects by optimization. The output is a NeRF that is trained by optimizing for rendered views to have high semantic similarity, given the text prompt. The method uses CLIP in synergy with geometric priors. DreamFusion [35] leverages powerful text-to-image diffusion models (here Imagen [43]) and introduces Score Distillation Sampling (SDS) to exploit diffusion priors as losses for 3D object optimization, an approach also adopted in [51]. Our work is related to CLIP-Forge [44], which trains a normalizing flow network to learn the mapping between the CLIP and the latent space of a 3D shape model, learned over a collection of 3D rigid objects.

3D Animal Models Three-dimensional differentiable articulated shape models have been defined for a few common species. SMAL [64] is a multi-species model that can represent a wide range of quadrupeds. SMALR [63] extends SMAL to capture 3D shapes of animals from a set of images. SMALST [62] learns a 3D model for the Gravy’s zebra from images. AVES [52] learns 3D shape of birds from images, starting from a reference template. hSMAL [23] and D-SMAL [41] are 3D parametric shape models for horses and dogs, respectively. Many recent methods do not assume an existing reference template. Lassie [58] and Hi-Lassie [59] create 3D models from a small collection of images. Like SMALR [63], they require different images with a clear, non occluded view of the animal. Artic3D [60] supports noisy images. Leopard [27] reconstructs 3D animals from images using a part-based neural representation. While applicable to animals with a different number of body parts, these methods do not reconstruct realistic fine-grained details, as the synthesis losses are based on matching silhouettes or image features. Moreover, they only reconstruct single animal instances. Methods exist to learn category-specific shape priors from images: MagicPony [55] learns models for horses, 3D-Fauna [25] extends the approach to arbitrary quadrupeds. RAC [57] learns category-level 3D models from video. GART [21] learns a subject specific model from monocular video.

3D Arboreal Trees Generation The modeling of trees and vegetation has a long history. Early approaches focused on modeling the branching structure, using fractals [1, 32], grammars and particle systems [17] and L-systems [36], with the latter proved effective to modeling a large variety of realistic trees, given a set of production rules. Weber and Penn [53] define a procedural model that, instead

of accurately modeling how trees grow, has a focus on the tree global geometry. Using such systems is complicated, requires a lot of knowledge to define a non-intuitive set of parameters. Recent methods exploit learning systems to easily define parameters, and automate the synthetic tree generation process. The recent DeepTree [61] learns rules from traditional procedural methods, and define a network that is able to automatically grow trees taking into account environment constraints. Lee et al. [20] train a neural network to generate parameters for procedural tree generation. None of these methods allow obtaining parameters from text, like we do. Li et al. [22] grow tree branches using a multi-cylindrical shape, estimated from an image mask, as surface limit.

3 Method

3.1 Animal Model

The SMAL⁺ parametric animal model is an extension of SMAL [64]. SMAL is defined by a triangular mesh template \mathbf{v}_t , with n_V vertices, a matrix B of shape $3n_V \times n_B$ containing the n_B basis vectors of a linear shape deformation space, a joint regressor J_r that maps model vertices to a set of n_J joint locations, and a skinning weight matrix W . An animal is generated, given shape parameters β and pose parameters θ , by first deforming the template into an intrinsic shape \mathbf{v}_s , then applying Linear Blend Skinning (LBS) to rotate the body parts according to the given pose:

$$\begin{aligned}\mathbf{v}_s &= \mathbf{v}_t + B\beta^T \\ \mathbf{v} &= LBS(\mathbf{v}_s, \theta; W, J_r).\end{aligned}\tag{1}$$

The linear shape space is learned with Principal Component Analysis (PCA) on a set of 41 quadruped toy scans. The SMAL⁺ we introduce here is obtained by leveraging the training samples of SMAL, D-SMAL [41] and hSMAL [23]. We register the training horses of the hSMAL model plus additional horse toy scans to the SMAL topology, obtaining a set of 60 registrations. We also add new species: Giraffe, Bear, Mouse, and Rat. We then learn an animal model on a total of 145 animals. Note that D-SMAL defines dog breeds for the training samples, while in hSMAL the breed of the training horses is undefined. After learning, we collect the set of shape variables for all the training samples, with their associated species or, in the case of dogs, breed name. This constitutes the training set for the AWOL animal shape prediction.

3.2 Tree Model

The tree model corresponds to the TreeGen add-on for Blender [13]. Tree-Gen procedurally generates realistic 3D models of trees on the basis of the method proposed by Weber and Penn [53] and exploiting the Blender’s Bézier curve system. The add-on supports saving the generated tree as a triangular mesh. The model generation is controlled by a set of parameters. Some of the parameters are



Fig. 2: Training set for the tree network. From left: Poplar, Maple, Palm, Silver Birch, English Oak, European Larch, Weeping Willow, Balsam Fir, Black Tupelo, Sphere Tree, Black Oak, Hill Cherry, Sassafras, Douglas Fir, Apple, Willow, Cypress, Magnolia, Pine, Fan Palm, Quaking Aspen.

categorical, referring to a set of defined tree or leaf shapes, and some are numerical, controlling the branches and leaves density. In addition, ranges of variation for the numerical parameters are also defined, such that the add-on can generate diverse results for the same set of reference parameters. Tree-Gen provides reference parameters labeled with the species name for a set of representative tree shapes. We add to the reference trees the Italian Cypress and Magnolia. This extended set of parameters and tree names constitutes the training set for the AWOL tree shape prediction (Fig. 2).

3.3 Text-to-Shape Model

We base our approach on the real-valued non-volume preserving (Real-NVP) model [6]. Real-NVP is a generative probabilistic model specifically designed for high-dimensional and highly structured data. Being formulated with a set of stably invertible transformations, and allowing exact and efficient reconstruction, Real-NVP is particularly suited for our task of latent space mapping with limited training data. We summarize Real-NVP here. Let $x \in X$ be an observed, high-dimensional variable, and $z \in Z$ a latent variable, with an associated simple prior distribution p_Z . Let f be a bijection $f : X \rightarrow Z$, with $f^{-1} = g : Z \rightarrow X$. Using the change of variable formula, a model on x can be defined as:

$$p_X(x) = p_Z(f(x)) \left| \det \left(\frac{\partial f(x)}{\partial x^T} \right) \right|, \quad (2)$$

where the determinant is computed over the Jacobian of f . In order to generate samples from $p_X(x)$ one would first sample a latent variable z from p_Z , then compute $x = g(z)$. Obtaining the density at x requires computing the Jacobian (Eq. 2). Dinh et al. [6] introduce a convenient construction of f using a set of bijective functions that are easy to invert. They formulate f in a way that its Jacobian is a triangular matrix, allowing for the determinant computation as the product of the diagonal terms. Specifically, f is obtained by stacking a set of *Affine Coupling Layers*. Each coupling layer computes a transformation from the input $x \in \mathbb{R}^D$ to the output $y \in \mathbb{R}^D$ as follows:

$$\begin{aligned} y_{1:d} &= x_{1:d} \\ y_{d+1:D} &= x_{d+1:D} \odot \exp(s(x_{1:d})) + t(x_{1:d}), \end{aligned} \quad (3)$$

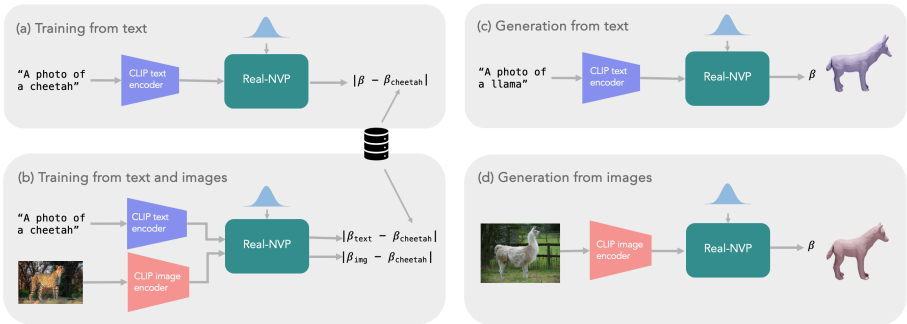


Fig. 3: Network architecture. At training, we can consider only text as input (a), or also provide reference images (b), with about 3 – 10 examples for each breed/species. At inference, we can query the text-only network with text (c), or the text-and-image network with images (d).

where $d < D$ and $s()$ and $t()$ are scale and translation functions that convert the input into a vector of dimension $D - d$. These transformations are easy to invert, and obtaining the Jacobian does not require computing derivatives for the scale and translation function [6]. The partitioning of the input vectors can be modeled with a binary mask. In [6] two strategies are considered: checkerboard masking and dimension-wise masking. In AWOL we employ Real-NVP to model the conditional distribution of the shape parameters (either shape variables β in SMAL⁺ or the parameters of the tree Blender add-on), given the CLIP encoding of the textual or visual input. Following [44], we define the input variable x in Eq. 3 as the concatenation between the CLIP encoding and the shape parameters. The output variable z is a unit Gaussian distribution. We adopt the Real-NVP model with important differences. First, instead of considering a fix masking like in previous work [6, 44], we consider trainable masks. Second, differently from the original formulation [6] and ClipForge [44], we seek for data reconstruction during training, employing a reconstruction loss, rather than a density estimation loss. This approach has been proved effective for training generative diffusion models [48]. We compare the different training losses in our ablation studies. As reconstruction loss, we use the $L1$ norm between predicted and ground truth shape parameters (See Fig. 3). Note that, during development, we also considered a $L2$ loss, with poor results. Finally, we follow previous work in defining simple small networks to implement the scale and translation functions, namely two Multi Layer Perceptron (MLP) networks. Differently from previous work, we add two additional fully-connected layers that compress the hidden space of those functions. We found that this compression layer is necessary when learning the binary masks, while it hurts performance when the traditional masking approaches are considered. We show the advantages of our design choices in our experiments.



Fig. 4: Dog breeds. We verify that CLIP can discriminate the dog breeds in the D-SMAL training set by running a zero-shot classification test on the images above, which achieved 100% accuracy.

4 Experiments

We first verify that CLIP can understand and discriminate between the different dog breeds and tree species. We consider an image for each of the dog breeds in the D-SMAL model (see Fig. 4), and perform zero-shot classification using the prompt "A photo of a <breed> dog". We found that CLIP can recognize all our training breeds. Interestingly, the Chevalier King Charles Spaniel is correctly detected only if indicated as King Charles Spaniel. We perform a similar experiment for our training tree species (Fig. 2) and a set of representative horse breeds (see Fig. 5). We found that the most distinctive trees are correctly recognized, while the majority of the horse breeds cannot be identified, except for ponies and big horses. Therefore, we identify such cases in our animal training set, and assign corresponding labels, while the remaining horses are generically labeled as "Horse".

4.1 Implementation

We implement the AWOL network in Pytorch. We define a single network for both the animal and tree data, with similar training parameters, and the main difference being the dimension of the shape space. The latent shape space for the animal network is the 145-dimensional space of the SMAL⁺ model. The values of the shape variables are Gaussian distributed with zero mean and identity



Fig. 5: Horse breeds. We found with a zero-shot classification test that among the horse breeds above, CLIP can correctly recognize only for the Tinker/Shire horses (violet box) and the Icelandic/Welsh ponies (blue box).

variance by construction. The latent space for the tree network corresponds to the parameters of the Blender add-on for tree generation. We set the parameters that define the degree of randomness to zero, and we consider, to define the latent space, only parameters that vary across the reference species. This leaves a latent space with 60 parameters out of the 105 defined by Tree-Gen. We center and normalize the variables by subtracting the mean and dividing by the standard deviation, such that the animals and tree parameters are defined with similar ranges. We do not apply the centering and normalization to the categorical variables, that we represent instead with a one-hot encoding. We consider 5 affine coupling layers, the hidden space for the scale and translation networks has dimension 1024, that we compress to 512 with an additional layer. We encode the text of the sentence "A photo of a <animal>" and "A photo of a <species> tree" for the animal and tree networks, respectively. We train the animal and tree networks on the text and shape data for 6000 epochs, which corresponds to a stabilization of the loss. We then train the same networks on text and images (Fig. 3 (b)). To do so, we download from the Web³ a set of images, between 3 to 10 for each tree/animal species or breed, and create training tuples composed by the CLIP image encoding and parameters. The training data is larger than previously, and we train the networks for 3000 epochs, which corresponds to a stabilization of the loss. Batch size is 16. We use the Adam optimizer with a learning rate that varies from $1e-4$ to $1e-6$. We use CLIP ViT-B/32-LAION-2B [15].



Fig. 6: Tree prediction from text. The generated tree species are, from left: Gingko, Coconut, Cedar of Lebanon, Fig, Cocoa, Bigleaf Maple, Deodar Cedar, Eucalyptus, Tulip, Oak, Banyan, American Elm, Acer, Coast Redwood, Sequoia, Western Red Cedar, White Spruce. None of these species is in the tree training set.

4.2 Evaluation

We evaluate our AWOL method in two settings: interpolation and generalization. **Interpolation.** We consider as interpolation task the prediction of new breeds for the dog class. In nature, dogs of different breeds can mix, and many breeds have been created by mixing existing ones [9]. We argue that, given the large number of breeds included in the model, it is likely that new breeds shapes can be generated by interpolation in the space of dog shapes, even if it is true that there could be unseen breeds with specific shape features not seen during training. We qualitatively demonstrate interpolation by generating dog breeds

³ <https://commons.wikimedia.org/>

	CLIP-based Comparison: % of votes			
	All	p-value	Dogs	Other Species
A. Check vs. Dims	61:39	0.19	68:32	43:57
B. Dims vs. Dims + Comp.	52:48	0.47	51:49	54:46
C. Check vs. Check. + Comp.	63:37	0.20	64:36	60:40
D. Learn + Comp. vs. Learn	61:39	0.19	59:41	69:31
E. Learn + Comp., 145 vs. 40	50:50	0.58	48:52	54:46
F. Learn + Comp. vs. Dims	62:38	0.13	68:32	46:54
G. Learn + Comp vs. Check	54:46	0.38	53:47	57:43
H. Learn + Comp, density loss	86:14	1.24e-7	86:14	86:14

Table 1: Ablation results. Comparison between different networks. Check is checkerboard masking, Dims is dimension-wise masking, Comp is hidden space compression, Learn is learned masks. (E) compares the Learn + Comp network with 145 (default) versus 40 shape parameters. The table show that the best performance on the whole testset is for the network with learned mask and compression (D, F, G). When training with also a density loss [6], performance degrades significantly.

in comparison with BITE [41] (Fig. 13). We also show interpolation for age and size. We query for "Giant Schnauzer", "Standard Schnauzer", "Miniature Schnauzer" and "Toy Schnauzer", and similarly for the Poodle. Note in Figure 12 how the network correctly predicts the scale of the different varieties of the breeds (it is worth noting that for the Schnauzer, the breed varieties are only Giant, Standard and Miniature). We then investigate if AWOL can interpolate shapes and age-dependent features by querying for "Baby", "Young", "Adult" and "Old" animals. Figure 12 shows the results for seen and unseen species. Figure 8 shows an analogous analysis for trees. We quantitatively compare the dog breed predictions from textual input with BITE [41] with a perceptual study. For each breed in the StanfordExtra testset [2], we generate a 3D dog, and compare with the dog reconstructed by BITE on a randomly selected image of the same breed. We let Amazon Mechanical Turk workers to judge which method better represents the dog breed in the picture. On the whole set, BITE outperforms AWOL with 971 vs 884 votes, as confirmed by a binomial test, with a p-value of 0.02 (BITE better than AWOL). We noticed that the task favors BITE when the subject in the image is a puppy, given AWOL used without age input generates an adult subject. By removing from the evaluation the images with baby dogs, we obtain votes of 830 (BITE) vs. 850 (AWOL), with a p-value of 0.3 (AWOL better than BITE), indicating the ability of AWOL to faithfully generate a large variety of breeds. **Generalization.** In order to test generalization, we prompt the model for creating new quadruped species. Figure 9 shows examples of generation from text. We show examples of reconstructed novel trees from textual and image input in Figure 6 and Figure 7, respectively. Finally, Figure 11 shows examples of generation of animals from images, where many are taken from [63], for comparison. Here the unseen animals are the Llama, Thylacine, Panda, Pig, Rhino, Cougar. Figure 10 shows a comparison with DeepTree [61].

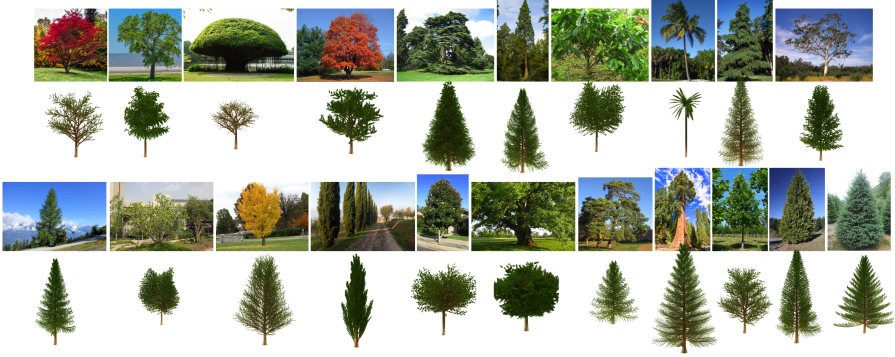


Fig. 7: Tree prediction from images. For each row: the input image and below the generated tree. Note that we do not predict the tree colors, and we show all the trees with an average green.

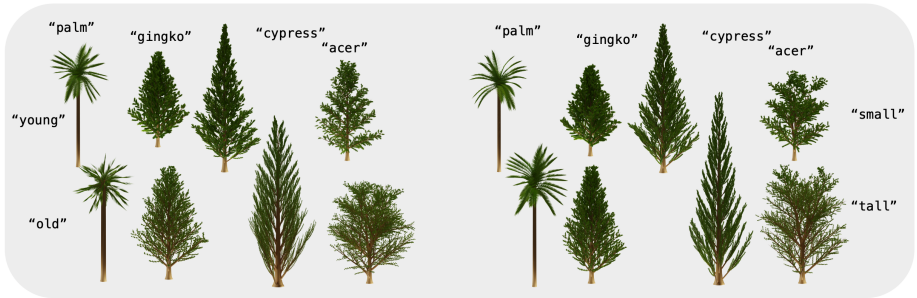


Fig. 8: Age and size interpolation for trees. Palm and Cypress are in the AWOL training set, while Gingko and Acer are unseen species. Here the query is "A photo of a <age> <species> tree".

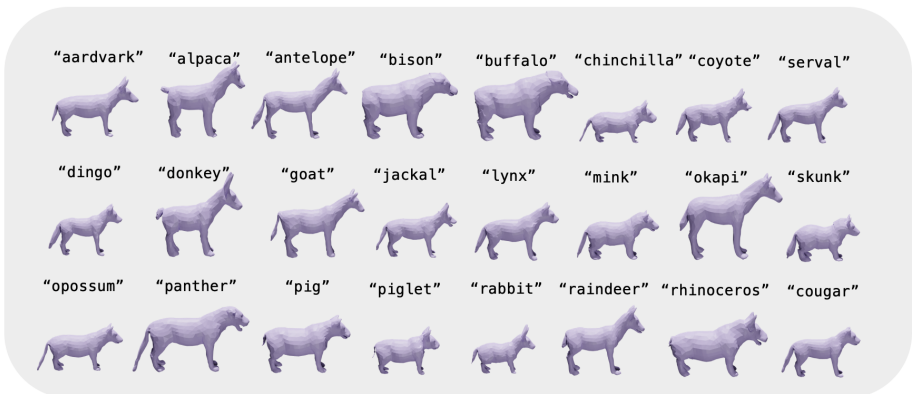


Fig. 9: Animals prediction from text. We generate species that are not present in the SMAL⁺ and AWOL training sets. The image shows the actual model size.

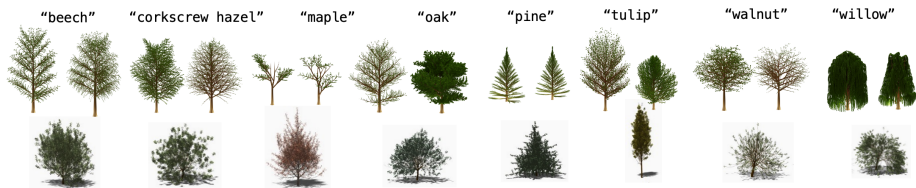


Fig. 10: Comparison with DeepTree. We show predicted trees from text (top), compared with DeepTree (bottom, images taken from [61]). For each predicted pair: (left) network trained only on text, (right) network trained on text and images.

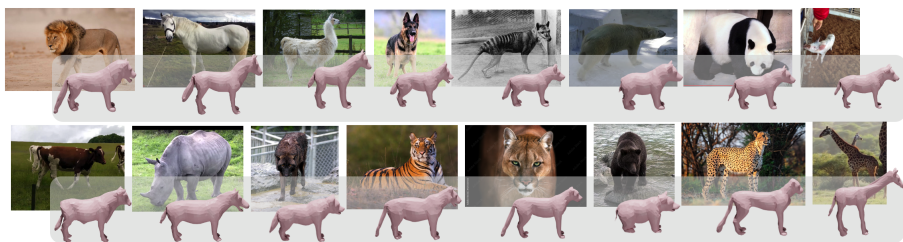
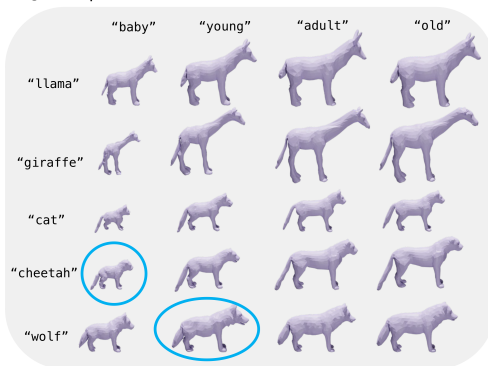


Fig. 11: Animals prediction from images. The Horse, Dog, Thylacine, Polar Bear, Panda, Pig, Cow, Rhino and Bear images are taken from [63]. We replace their green screen images with natural images for the Lion, Tiger, Cougar and Cheetah.

Age interpolation



Size interpolation

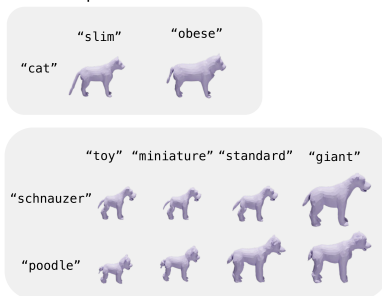


Fig. 12: Age interpolation (left) and size interpolation (right). The circles indicate the animals that are present in the training set as "Baby Cheetah" and "Young Wolf". Giraffe, Cat, and Wolf are in the training set without attributes, while the Llama is not. The small and large Poodles are present in the training set with text attribute is "Poodle". Only one shape example for the Schnauzer is present, named "Schnauzer". Note how we can recover the different Poodle breed size variations. For the Schnauzer, the actual breed variations are Miniature, Standard and Giant.

4.3 Ablation Studies

We perform our ablation studies on the animal model. We use CLIP for evaluation, as we found that CLIP can successfully classify animals and dog breeds in particular, allowing quantitative testing on a larger set of cases. We perform ablation studies to evaluate: the effect of learning the binary masks in Real-NVP; the effect of training with a density loss; the effect of adding the compression layer in the scale and translation functions. We also compare with reducing the shape space dimension from 145, the space of the SMAL⁺ model, to a dimension of 40, approximately matching the dimension of the dogs and horses single SMAL models [41] [23]. We generate a set of 122 animals, none of them present in the SMAL⁺ model training set. This selection covers most of the common quadrupeds, and several unseen dog breeds. We query the network with the sentence "A photo of a <animal name>", where <animal name> is either a quadruped species or dog breed. We then render the predicted 3D models in grayscale, in order to prevent any color bias. Given the networks can predict different animal sizes, we consider bounding boxes. We render the animals to maximize visibility of their profile. We found that the lateral view is the most informative, while adding further views gave inconsistent results. We perform paired comparison between different networks by testing, for each animal, which of the two networks predictions, encoded in CLIP, is closest to the CLIP encoding of the animal name. This corresponds to a CLIP "vote". Note that, even if we base our method on CLIP, we believe it is appropriate to use CLIP for the ablation studies, as we are comparing different architectures, under the same conditions. Results are reported in Table 1. Our ablation studies confirm that the network with learned masks and compression of the hidden space for the scale and translation networks provides the best performance on the whole testset.

5 Conclusion

We have addressed the problem of generating 3D objects from text and images using parametric 3D models. Inspired by recent work on learning multimodal latent spaces, we use language to control the selection of the 3D models parameters. We make the hypothesis that using language we can achieve interpolation and generalization in parametric shape spaces. We demonstrate our hypothesis on two different 3D generative models: on a novel differentiable 3D parametric shape model for animals, that extends previous models with new training samples and species, and on a non-differentiable model for trees, represented by a Blender add-on. Our qualitative and quantitative experiments confirm our hypothesis. The proposed AWOL is the first system that allows generating rigged 3D animals and trees with a simple text prompt. **Acknowledgements.** We thank Tsvetelina Alexiadis, Taylor McConnell and Tomasz Niewiadomski for the huge help in running the Amazon Mechanical Turk evaluation. We also thank Charlie Hewitt for making his tree generation method available and the authors of [44] for sharing their code.

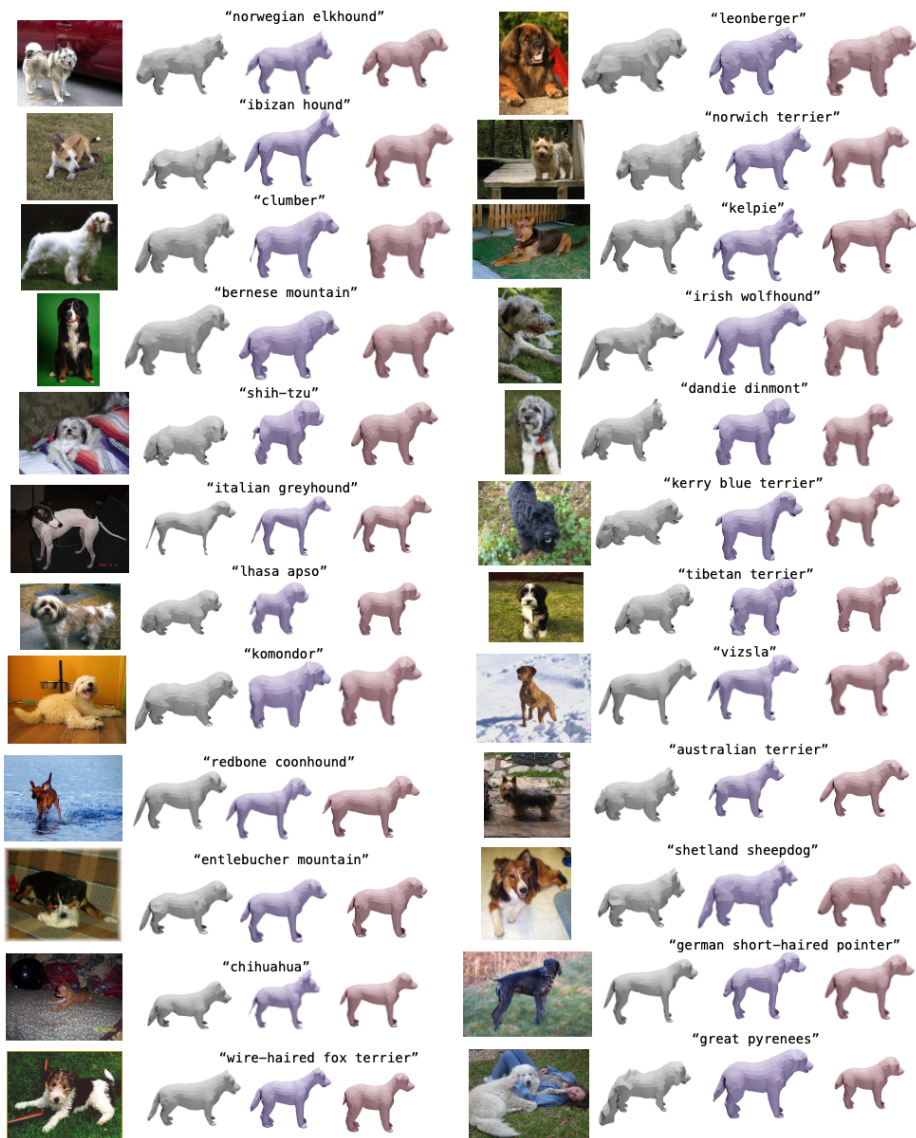


Fig. 13: Comparison with BITE [41]. Randomly chosen images from the StanfordExtra testset. From left: input image, BITE result rendered in a natural pose (gray), AWOL result with textual input (purple), AWOL result with image input (red). For BITE and AWOL with text input, we use the breed label to rotate the ears. For AWOL from images, ears are down by default. None of these breeds are in the AWOL training set.

References

1. Aono, M., Kunii, T.L.: Botanical tree image generation. *IEEE Computer Graphics and Applications* 4(5), 10–34 (1984). <https://doi.org/10.1109/MCG.1984.276141>
2. Biggs, B., Boyne, O., Charles, J., Fitzgibbon, A., Cipolla, R.: Who left the dogs out: 3D animal reconstruction with expectation maximization in the loop. In: *ECCV*. pp. 195–211 (2020)
3. Bogo, F., Kanazawa, A., Lassner, C., Gehler, P., Romero, J., Black, M.J.: Keep it SMPL: Automatic estimation of 3D human pose and shape from a single image. In: *Computer Vision – ECCV 2016. Lecture Notes in Computer Science*, Springer International Publishing (Oct 2016)
4. Cheng, Y.C., Lee, H.Y., Tulyakov, S., Schwing, A., Gui, L.: SDFusion: Multimodal 3d shape completion, reconstruction, and generation. In: *Conference on Computer Vision and Pattern Recognition (CVPR)* (2023)
5. Choutas, V., Müller, L., Huang, C.H.P., Tang, S., Tzionas, D., Black, M.J.: Accurate 3d body shape regression using metric and semantic attributes. In: *2022 IEEE/CVF Conference on Computer Vision and Pattern Recognition (CVPR 2022)*. pp. 2708–2718. IEEE, Piscataway, NJ (Jun 2022). <https://doi.org/10.1109/CVPR52688.2022.00274>
6. Dinh, L., Sohl-Dickstein, J., Bengio, S.: Density estimation using real nvp. In: *ICLR* (2017)
7. Dwivedi, S.K., Athanasiou, N., Kocabas, M., Black, M.J.: Learning to regress bodies from images using differentiable semantic rendering. In: *Proc. International Conference on Computer Vision (ICCV)*. pp. 11230–11239. IEEE, Piscataway, NJ (Oct 2021). <https://doi.org/10.1109/ICCV48922.2021.01106>
8. Feng, Y., Choutas, V., Bolkart, T., Tzionas, D., Black, M.J.: Collaborative regression of expressive bodies using moderation. In: *2021 International Conference on 3D Vision (3DV 2021)*. pp. 792–804. IEEE, Piscataway, NJ (Dec 2021). <https://doi.org/10.1109/3DV53792.2021.00088>
9. G., P.H., L., D.D., M., R., W., D.B., B., M.A., G., C.R., A., O.E.: Genomic analyses reveal the influence of geographic origin, migration, and hybridization on modern dog breed development. *Cell Reports* 4(19), 697–708 (2017)
10. Ge, S., Park, T., Zhu, J.Y., Huang, J.B.: Expressive text-to-image generation with rich text. In: *Proceedings of the IEEE/CVF International Conference on Computer Vision (ICCV)*. pp. 7545–7556 (October 2023)
11. Goel, S., Pavlakos, G., Rajasegaran, J., Kanazawa*, A., Malik*, J.: Humans in 4D: Reconstructing and tracking humans with transformers. In: *International Conference on Computer Vision (ICCV)* (2023)
12. Gralnik, O., Gafni, G., Shamir, A.: Semantify: Simplifying the control of 3d mophable models using clip. In: *Proceedings of the IEEE/CVF International Conference on Computer Vision (ICCV)*. pp. 14554–14564 (October 2023)
13. Hewitt, C.: Procedural generation of tree models for use in computer graphics (2017), <https://github.com/friggog/tree-gen>
14. Hu, J., Hui, K.H., Liu, Z., Zhang, H., Fu, C.W.: Clipxplore: Coupled clip and shape spaces for 3d shape exploration. In: *SIGGRAPH Asia 2023 Conference Papers*. SA '23, Association for Computing Machinery, New York, NY, USA (2023). <https://doi.org/10.1145/3610548.3618144>, <https://doi.org/10.1145/3610548.3618144>

15. Ilharco, G., Wortsman, M., Wightman, R., Gordon, C., Carlini, N., Taori, R., Dave, A., Shankar, V., Namkoong, H., Miller, J., Hajishirzi, H., Farhadi, A., Schmidt, L.: Openclip (Jul 2021). <https://doi.org/10.5281/zenodo.5143773>, <https://doi.org/10.5281/zenodo.5143773>, if you use this software, please cite it as below.
16. Jain, A., Mildenhall, B., Barron, J.T., Abbeel, P., Poole, B.: Zero-shot text-guided object generation with dream fields. In: Conference on Computer Vision and Pattern Recognition (CVPR) (2022)
17. Jain, A., Sunkara, J., Shah, I., Sharma, A., Rajan, K.S.: Automated tree generation using grammar & particle system. In: Proceedings of the Twelfth Indian Conference on Computer Vision, Graphics and Image Processing. ICVGIP '21, Association for Computing Machinery, New York, NY, USA (2021). <https://doi.org/10.1145/3490035.3490285>, <https://doi.org/10.1145/3490035.3490285>
18. Kocabas, M., Huang, C.H.P., Hilliges, O., Black, M.J.: PARE: Part attention regressor for 3D human body estimation. In: Proc. International Conference on Computer Vision (ICCV). pp. 11107–11117. IEEE, Piscataway, NJ (Oct 2021). <https://doi.org/10.1109/ICCV48922.2021.01094>
19. Kocabas, M., Huang, C.H.P., Tesch, J., Müller, L., Hilliges, O., Black, M.J.: SPEC: Seeing people in the wild with an estimated camera. In: Proc. International Conference on Computer Vision (ICCV). pp. 11015–11025. IEEE, Piscataway, NJ (Oct 2021). <https://doi.org/10.1109/ICCV48922.2021.01085>
20. Lee, J.J., Li, B., Benes, B.: Latent l-systems: Transformer-based tree generator. *ACM Trans. Graph.* **43**(1) (nov 2023). <https://doi.org/10.1145/3627101>, <https://doi.org/10.1145/3627101>
21. Lei, J., Wang, Y., Pavlakos, G., Liu, L., Daniilidis, K.: Gart: Gaussian articulated template models (2023)
22. Li, B., Kałużny, J., Klein, J., Michels, D.L., Pałubicki, W., Benes, B., Pirk, S.: Learning to reconstruct botanical trees from single images. *ACM Trans. Graph.* (2021). <https://doi.org/10.1145/3478513.3480525>, <https://doi.org/10.1145/3478513.3480525>
23. Li, C., Ghorbani, N., Broomé, S., Rashid, M., Black, M.J., Hernlund, E., Kjellström, H., Zuffi, S.: hsmal: Detailed horse shape and pose reconstruction for motion pattern recognition. arXiv preprint arXiv:2106.10102 (2021). <https://doi.org/https://doi.org/10.48550/arXiv.2106.10102>
24. Li, M., Zhou, P., Liu, J.W., Keppo, J., Lin, M., Yan, S., Xu, X.: Instant3d: Instant text-to-3d generation. arxiv: 2311.08403 (2023)
25. Li, Z., Litvak, D., Li, R., Zhang, Y., Jakab, T., Rupprecht, C., Wu, S., Vedaldi, A., Wu, J.: Learning the 3d fauna of the web. arXiv preprint arXiv:2401.02400 (2024)
26. Lin, C.H., Gao, J., Tang, L., Takikawa, T., Zeng, X., Huang, X., Kreis, K., Fidler, S., Liu, M.Y., Lin, T.Y.: Magic3d: High-resolution text-to-3d content creation. In: CVPR (2023)
27. Liu, D., Stathopoulos, A., Zhangli, Q., Gao, Y., Metaxas, D.: Leopard: Learning explicit part discovery for 3d articulated shape reconstruction. In: NeurIPS (2023)
28. Loper, M., Mahmood, N., Romero, J., Pons-Moll, G., Black, M.J.: SMPL: A skinned multi-person linear model. *ACM Trans. Graphics (Proc. SIGGRAPH Asia)* **34**(6), 248:1–248:16 (Oct 2015)
29. Lorraine, J., Xie, K., Zeng, X., Lin, C.H., Takikawa, T., Sharp, N., Lin, T.Y., Liu, M.Y., Fidler, S., Lucas, J.: Att3d: Amortized text-to-3d object synthesis. In: Proceedings of the IEEE/CVF International Conference on Computer Vision (ICCV). pp. 17946–17956 (October 2023)

30. Mildenhall, B., Srinivasan, P.P., Tancik, M., Barron, J.T., Ramamoorthi, R., Ng, R.: Nerf: representing scenes as neural radiance fields for view synthesis. *Commun. ACM* **65**(1), 99–106 (dec 2021). <https://doi.org/10.1145/3503250>, <https://doi.org/10.1145/3503250>
31. Müller, L., Ye, V., Pavlakos, G., Black, M.J., Kanazawa, A.: Generative proxemics: A prior for 3D social interaction from images. *arXiv preprint 2306.09337v2* (2023)
32. Oppenheimer, P.E.: Real time design and animation of fractal plants and trees. In: *Proceedings of the 13th Annual Conference on Computer Graphics and Interactive Techniques*. p. 55–64. SIGGRAPH '86, Association for Computing Machinery, New York, NY, USA (1986). <https://doi.org/10.1145/15922.15892>, <https://doi.org/10.1145/15922.15892>
33. Pavlakos, G., Malik, J., Kanazawa, A.: Human mesh recovery from multiple shots. In: *CVPR* (2022)
34. Pavlakos*, G., Weber*, E., Tancik, M., Kanazawa, A.: The one where they reconstructed 3d humans and environments in tv shows. In: *ECCV* (2022)
35. Poole, B., Jain, A., Barron, J.T., Mildenhall, B.: DreamFusion: Text-to-3d using 2d diffusion. In: *International Conference on Learning Representations (ICLR)* (2023)
36. Prusinkiewicz, P., Lindenmayer, A.: *Graphical modeling using L-systems*, pp. 1–50. Springer New York, New York, NY (1990). https://doi.org/10.1007/978-1-4613-8476-2_1, https://doi.org/10.1007/978-1-4613-8476-2_1
37. Radford, A., Kim, J.W., Hallacy, C., Ramesh, A., Goh, G., Agarwal, S., Sastry, G., Askell, A., Mishkin, P., Clark, J., Krueger, G., Sutskever, I.: Learning transferable visual models from natural language supervision. In: Meila, M., Zhang, T. (eds.) *Proceedings of the 38th International Conference on Machine Learning*. *Proceedings of Machine Learning Research*, vol. 139, pp. 8748–8763. PMLR (18–24 Jul 2021), <https://proceedings.mlr.press/v139/radford21a.html>
38. Ramesh, A., Dhariwal, P., Nichol, A., Chu, C., Chen, M.: Hierarchical text-conditional image generation with clip latents (2022)
39. Ramesh, A., Pavlov, M., Goh, G., Gray, S., Voss, C., Radford, A., Chen, M., Sutskever, I.: Zero-shot text-to-image generation. In: Meila, M., Zhang, T. (eds.) *Proceedings of the 38th International Conference on Machine Learning*. *Proceedings of Machine Learning Research*, vol. 139, pp. 8821–8831. PMLR (18–24 Jul 2021), <https://proceedings.mlr.press/v139/ramesh21a.html>
40. Rombach, R., Blattmann, A., Lorenz, D., Esser, P., Ommer, B.: High-resolution image synthesis with latent diffusion models (2022)
41. Rüegg, N., Tripathi, S., Schindler, K., Black, M.J., Zuffi, S.: BITE: Beyond priors for improved three-D dog pose estimation. In: *IEEE/CVF Conf. on Computer Vision and Pattern Recognition (CVPR)*. pp. 8867–8876 (Jun 2023)
42. Ruiz, N., Li, Y., Jampani, V., Pritch, Y., Rubinstein, M., Aberman, K.: Dreambooth: Fine tuning text-to-image diffusion models for subject-driven generation. In: *CVPR* (2023)
43. Saharia, C., Chan, W., Saxena, S., Li, L., Whang, J., Denton, E., Ghasemipour, S.K.S., Gontijo-Lopes, R., Ayan, B.K., Salimans, T., Ho, J., Fleet, D.J., Norouzi, M.: Photorealistic text-to-image diffusion models with deep language understanding. In: Oh, A.H., Agarwal, A., Belgrave, D., Cho, K. (eds.) *Advances in Neural Information Processing Systems* (2022), <https://openreview.net/forum?id=08Ykn512A1>
44. Sanghi, A., Chu, H., Lambourne, J.G., Wang, Y., Cheng, C.Y., Fumero, M.: Clipforge: Towards zero-shot text-to-shape generation. In: *CVPR*. *IEEE Computer Society* (2022)

45. Streuber, S., Quiros-Ramirez, M.A., Hill, M.Q., Hahn, C.A., Zuffi, S., O’Toole, A., Black, M.J.: Body Talk: Crowdshaping realistic 3D avatars with words. *ACM Trans. Graph. (Proc. SIGGRAPH)* **35**(4), 54:1–54:14 (Jul 2016)
46. Sun, Y., Bao, Q., Liu, W., Fu, Y., Black, M.J., Mei, T.: Monocular, one-stage, regression of multiple 3D people. In: *Proc. International Conference on Computer Vision (ICCV)*. pp. 11159–11168. IEEE, Piscataway, NJ (Oct 2021). <https://doi.org/10.1109/ICCV48922.2021.01099>
47. Sun, Y., Bao, Q., Liu, W., Mei, T., Black, M.J.: TRACE: 5D temporal regression of avatars with dynamic cameras in 3D environments. In: *IEEE/CVF Conf. on Computer Vision and Pattern Recognition (CVPR)*. pp. 8856–8866 (Jun 2023)
48. Tevet, G., Raab, S., Gordon, B., Shafir, Y., Cohen-or, D., Bermano, A.H.: Human motion diffusion model. In: *The Eleventh International Conference on Learning Representations (2023)*, <https://openreview.net/forum?id=SJ1kSy02jwu>
49. Tripathi, S., Müller, L., Huang, C.H.P., Omid, T., Black, M.J., Tzionas, D.: 3D human pose estimation via intuitive physics. In: *Conference on Computer Vision and Pattern Recognition (CVPR)*. pp. 4713–4725 (2023), <https://ipman.is.tue.mpg.de>
50. Tsalicoglou, C., Manhardt, F., Tonioni, A., Niemeyer, M., Tombari, F.: Textmesh: Generation of realistic 3d meshes from text prompts. In: *International conference on 3D vision (3DV)* (2024)
51. Wang, H., Du, X., Li, J., Yeh, R.A., Shakhnarovich, G.: Score jacobian chaining: Lifting pretrained 2d diffusion models for 3d generation. In: *CVPR* (2023)
52. Wang, Y., Kolotouros, N., Daniilidis, K., Badger, M.: Birds of a feather: Capturing avian shape models from images. In: *CVPR* (2021)
53. Weber, J., Penn, J.: Creation and rendering of realistic trees. *ACM TOG* pp. 119–128 (1995)
54. Wu, M., Zhu, H., Huang, L., Zhuang, Y., Lu, Y., Cao, X.: High-fidelity 3d face generation from natural language descriptions. In: *Proceedings of IEEE/CVF Conference on Computer Vision and Pattern Recognition (CVPR)* (2023)
55. Wu, S., Li, R., Jakab, T., Rupprecht, C., Vedaldi, A.: Magicpony: Learning articulated 3d animals in the wild. In: *CVPR*. pp. 8792–8802 (June 2023)
56. Xu, J., Wang, X., Cheng, W., Cao, Y.P., Shan, Y., Qie, X., Gao, S.: Dream3D: Zero-shot text-to-3d synthesis using 3d shape prior and text-to-image diffusion models. <https://arxiv.org/abs/2212.14704> (2023)
57. Yang, G., Wang, C., Reddy, N.D., Ramanan, D.: Reconstructing animatable categories from videos. In: *CVPR*. pp. 16995–17005 (June 2023)
58. Yao, C.H., Hung, W.C., Li, Y., Rubinstein, M., Yang, M.H., Jampani, V.: Lassie: Learning articulated shape from sparse image ensemble via 3d part discovery. In: *NeurIPS* (2022)
59. Yao, C.H., Hung, W.C., Li, Y., Rubinstein, M., Yang, M.H., Jampani, V.: Hi-lassie: High-fidelity articulated shape and skeleton discovery from sparse image ensemble. In: *CVPR* (2023)
60. Yao, C.H., Raj, A., Hung, W.C., Li, Y., Rubinstein, M., Yang, M.H., Jampani, V.: Artic3d: Learning robust articulated 3d shapes from noisy web image collections. In: *NeurIPS* (2023)
61. Zhou, X., Li, B., Benes, B., Fei, S., Pirk, S.: Deeptree: Modeling trees with situated latents. *Transactions on Visualization & Computer Graphics* **1**, 1–14 (2023)
62. Zuffi, S., Kanazawa, A., Berger-Wolf, T., Black, M.J.: Three-D safari: Learning to estimate zebra pose, shape, and texture from images ”in the wild”. In: *ICCV*. pp. 5359–5368 (2019)

63. Zuffi, S., Kanazawa, A., Black, M.J.: Lions and tigers and bears: Capturing non-rigid, 3D, articulated shape from images. In: CVPR. pp. 3955–3963. IEEE Computer Society (2018)
64. Zuffi, S., Kanazawa, A., Jacobs, D., Black, M.J.: 3D menagerie: Modeling the 3D shape and pose of animals. In: CVPR (Jul 2017)